77-1340

Some Results of the Testing of a Full-Scale Ogee-Tip Rotor

Wayne R. Mantay*
Structures Laboratory—USARTL (AVRADCOM), Hampton, Va.

Phillip A. Shidler* and Richard L. Campbell*
NASA Langley Research Center, Hampton, Va.

Full-scale tests were utilized to investigate the effect of the Ogee tip on helicopter rotor acoustics, performance, and loads. Two facilities were used for this study: the Langley whirl tower and a UH-1H helicopter. The test matrix for hover on the whirl tower involved thrust values from 0 to 44,480 N (10,000 lb) at several tip Mach numbers for both standard and Ogee rotors. The full-scale testing on the UH-1H encompassed the major portion of the flight envelope for that aircraft. Both near-field acoustic measurements as well as far-field flyover data were obtained for both the Ogee and standard rotors. Data analysis of the whirl-tower test shows that the Ogee tip does significantly diffuse the tip vortex while providing some improvement in hover performance at moderate thrust coefficients. Flight testing of both rotors indicates that the strong impulsive noise signature of the standard rotor can be reduced with the Ogee rotor. Forward flight performance was significantly improved with the Ogee configuration for moderate lift coefficients. Further, rotor control loads and vibrations were reduced through use of this advanced tip rotor.

Nomenclature

a	= local speed of sound, m/s
C_L	= rotor lift coefficient, $GW/\rho\pi R^2(\Omega R)^2$
C_p	= engine power coefficient, $P/\rho\pi R^2(\Omega R)^3$
C_Q	= rotor torque coefficient, $Q/\rho\pi R^3(\Omega R)^2$
C_T	= rotor thrust coefficient, $T/\rho\pi R^2(\Omega R)^2$
GW	= helicopter gross weight, N (lb)
M_{TIP}	= rotor tip Mach number, $\Omega R/a$
n	= rotor load factor, g
OASPL	= overall sound pressure level, dB
P	= engine power, N-m/s
Q	= rotor torque, N-m
R	= rotor radius, m (ft)
R/D	= rate of descent, ft/min
T	= rotor thrust, N
V_T	= true airspeed, knots
ρ	= local air mass density, kg/m^3
Ω	= rotor rotational speed, rad/s

Superscript

$-$	= mean value

Introduction

THE high noise and vibration levels of the present-day helicopter reduce its usefulness and effectiveness. The increasing use of helicopters for military and commercial purposes necessitates a reduction in vibration as well as internal and external noise levels for reduced detection and community and passenger acceptance.

The interaction of a rotor blade tip vortex with the following blades is a major cause of increased helicopter acoustic signature, vibration, and loads.[1] Numerous methods of reducing this vortex-blade interaction have been investigated in the past. One method, tip-shape modification, has shown some promise in reducing the severity of this phenomenon. One of the more promising tip configurations is the Ogee planform (Fig. 1). Previous small-scale smoke studies indicated that this shape would diffuse the rotor blade tip vortex, and following blades might thus encounter a weaker vortex field with accompanying benefits. The Ogee-tip shape[1] was evaluated by a series of analytical and experimental programs.[2-5] Based on the encouraging results of the vortex flow data, pressure data, and performance information from these preliminary studies, full-scale testing of this tip shape was initiated.

Tests were conducted to investigate the effect of the Ogee tip on full-scale rotor acoustics, performance, and loads. The Langley whirl tower was utilized for hover flight measurements and an extensively instrumented UH-1H provided forward flight data.

Method of Approach

A systematic and controlled investigation of the effect of an advanced tip shape on rotor acoustics, loads, and performance was conducted on an Ogee-tip rotor and a standard UH-1H square-tip rotor. Test facilities used for this study included the NASA-Langley whirl tower, an instrumented UH-1H helicopter, and the acoustic range at NASA Wallops Flight Center. Both near- and far-field acoustic data were obtained, as well as rotor performance, loads data, and wake-flow visualization.

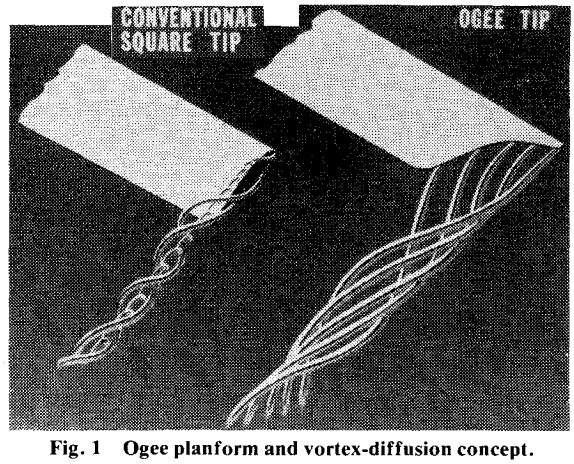

Fig. 1 Ogee planform and vortex-diffusion concept.

Presented as Paper 77-1340 at the AIAA 4th Aeroacoustics Conference, Atlanta, Ga., Oct. 3-5, 1977; submitted Oct. 11, 1977; revision received Aug. 9, 1978.

Index categories: Aeroacoustics; Helicopters; Testing, Flight and Ground.

*Aero-Space Technologist.

Table 1 Whirl-tower characteristics

Rotor height from ground	12.8 m (42 ft)
Available power	1.119 MW (1500 hp)
Type of rotor drive	electric motor

Table 2 Test rotor characteristics

	Standard	Ogee
Type of hub	Teetering	Teetering
Rotor radius	7.315 m (24 ft)	7.315 m (24 ft)
Blade chord	53.34 cm (21 in.) constant	53.34 cm (21 in.) varying
Blade airfoil	0012	0012
Blade twist (root to tip)	-10.9 deg linear	-10 deg
Precone angle	2.375 deg	2.375 deg
Number of blades	2	2
Rotor nominal rotational speed	324 rpm	324 rpm
Rotor solidity	0.04655	0.04412

Table 3 Whirl-tower instrumentation

Parameter	Sensor
Thrust	Load cells
Torque	Strain-gage bridge
Angular velocity	Photo counter
Thrust correction	Strain-gage bridge
Collective pitch angle	Potentiometer
Ambient temperature	Thermocouple
Static pressure	Barometer
Blade loads	Strain-gage bridges

Description of Test Facilities and Hardware

Whirl Tower

The Langley whirl tower has the capability of testing rotors through a complete hover envelope of thrust and rotational speed. The facility's characteristics are shown in Fig. 2 and Table 1. The tower was used to verify the structural integrity of the Ogee design as well as provide performance, acoustics, and flow visualization data.

Test Helicopter

The test vehicle for this investigation was a UH-1H helicopter. As shown in Fig. 3, the vehicle was equipped with electronic data systems, including an in-flight acoustic measurement system. Nominal test weights for the UH-1H were 33,805 N (7600 lb) and 38,253 N (8600 lb). The aircraft was flown with a crew of four resulting in a nominal longitudinal center of gravity location 17.8 cm (7 in.) aft of the main rotor hub.

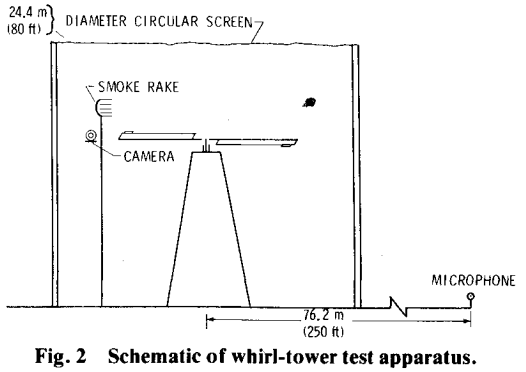

Fig. 2 Schematic of whirl-tower test apparatus.

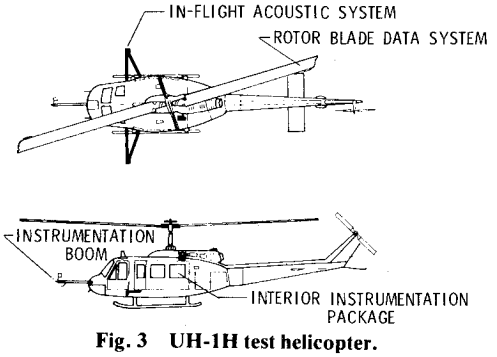

Fig. 3 UH-1H test helicopter.

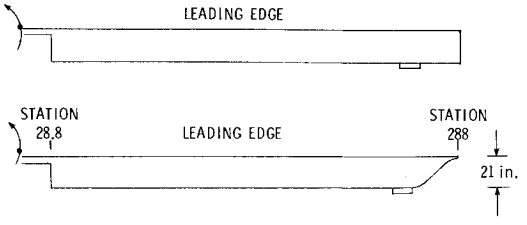

Fig. 4 Test rotor planforms.

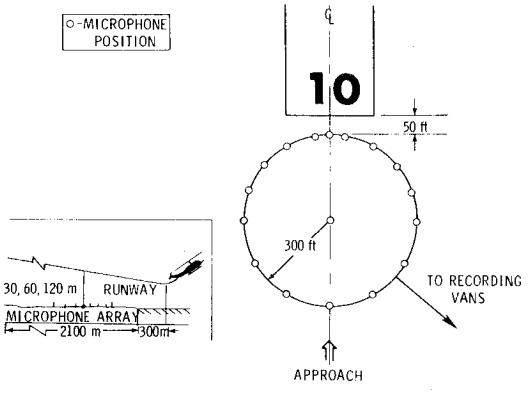

Fig. 5 Acoustic-array schematic.

Rotor Systems

The geometric characteristics of both standard and Ogee rotors used in the tests are given in Table 2. Two sets of each rotor were used, one set of each for the tower investigation and one set of each for flight testing on the instrumented helicopter. Figure 4 shows the planform of both the standard rotor and Ogee-tip rotor blades.

NASA Wallops Flight Center Acoustic Range

An acoustic array was used to measure far-field noise from the helicopter. This array was located at the approach end of runway 10. Radar was used to track the vehicle over the approach to the array.

Description of Instrumentation

Whirl-Tower Data Acquisition

The parameters directly measured by the whirl-tower data system are listed in Table 3. Performance data as well as blade-structural data were monitored in real time and recorded on FM tape. Acoustic data were obtained through a system identical to that used in the Wallops Flight Center acoustic instrumentation, to be discussed later in this paper, with one microphone placed 76.2 m (250 ft) from the center of the tower on a ground board.

Helicopter Instrumentation

The UH-1H helicopter utilized three unique data systems. One onboard data package recorded and telemetered select

Table 4 Flight data parameters

Parameter	Sensor	Data type	Accuracy, %[a]
Three vehicle attitudes	Gyro	PCM	1.0
Three angular rates	Gyro	PCM	1.0
Three linear accelerations	Accelerometer	PCM	1.0
Four control inputs	Transducer	PCM	1.0
Angle of attack	Vane/potentiometer	PCM	1.0
Angle of sideslip	Vane/potentiometer	PCM	1.0
Main rotor blade angle	Control position transducer	PCM	1.0
Main rotor azimuth	Shaft encoder	PCM	1.0
Total temperature	Hot wire	PCM	1.0
Static/differential pressure	Pressure transducer	PCM	1.0
Main rotor speed	Magnetic counter	PCM	1.0
Engine torque pressure	Pressure transducer	PCM	1.0
Rate of climb	Inertial vertical-speed indicator	PCM	1.0
Chordwise bending moment at stations 84 and 192 on main rotor blade	Strain gage	FM	2.5
Flapwise bending moment at stations 84 and 192 on main rotor blade	Strain gage	FM	2.5
Rotating pitch-link load	Strain gage	FM	2.5
Time code	36-bit time-code generator		
Ogee-tip joint bending moments	Strain gage	High-speed PCM	1.0
Ogee-tip pressures	Flush-mounted pressure transducers	High-speed PCM	1.0

[a] Full-scale.

helicopter parameters, which included vehicle aerodynamic state, attitudes, power train data, rotor-structural information, and vibratory loads. Table 4 lists these parameters and the measurement techniques used. A second onboard data system digitally sampled tip pressures, strain-gage information, and rotor azimuth on the Ogee rotor. The electronics of this system were embedded in the Ogee tip and enabled sampling rates as high as 2000 Hz to be obtained.

The in-flight acoustic measurement system (IFAMS) measured and recorded the near-field pressure signature of the test helicopter in various flight conditions. The system consists of two externally mounted microphones. The location of these microphones is shown in Fig. 3. The condenser microphones, fitted with a streamlined nose section, could be adjusted ± 10 deg. from centerline into the resultant local airflow. The microphone diaphrams were located 190 cm forward of the main rotor hub and 304 cm beneath it. The microphone booms extended 2.7 m from the centerline of the aircraft. The acoustic data from the IFAMS were recorded by two independent systems with a common 1-kHz time code.

Acoustic Array Instrumentation

A schematic diagram of the noise data-acquisition system for the flyover tests is shown in Fig. 5. During the test program, the microphones were fitted with wind screens and positioned 1.2 m above ground surface, oriented for grazing incidence. The condenser microphones in this array had a frequency response flat to within ±3 dB over the frequency range 10 to 20,000 Hz. The signal outputs from all microphones were recorded at each of the mobile data-acquisition stations on FM tape at 76.2 cm/s using a center frequency of 54 kHz. All recorded acoustic array data contained the same time code as the onboard data systems. The frequency of the complete acoustic system was flat to ±3 dB from 10 to 10,000 Hz.

Test Procedure

Evaluation of the Ogee-tip shape required a systematic and controlled test environment for the measurement of acoustic signature, rotor loads, and performance. The goal of the whirl-tower tests was to explore the hover envelope of both standard and Ogee rotors. The helicopter flight tests explored those conditions which created impulsive noise through blade-vortex interactions or compressibility. In both types of testing, simultaneous measurements of rotor loads and performance were made along with acoustic data acquisition.

Table 5 Whirl-tower hover test matrix

Thrust (N) lb		rpm 240	291	324[a]	356[b]
0		↓	↓	↓	↓
(8,896)	2,000	↓	↓	↓	↓
(17,792)	4,000	↓	↓	↓	↓
(26,688)	6,000	↓	↓	↓	↓
(35,584)	8,000	↓	↓	↓	↓
(44,480)	10,000	↓	↓	↓	↓

[a] Nominal aircraft operating rpm. [b] Ogee rotor only.

Table 6 Flight test envelope for near-field acoustic and systems data

IAS	Rate of descent, fpm	Flight condition
30,40	-25 to -200	Climb
20-120	0	Level flight
55-115	100 to 1500	Descent
50,60,80,90	0 (1.5g, 2.0g turns)	Maneuver
0	0 (in ground effect; out of ground effect)	Hover

Table 7 Flight conditions over acoustic array

IAS	Rate of descent, fpm
55, 80, 115	0
55, 70, 80, 90	100, 250, 350, 600, 1000

Whirl-Tower Test Procedure

The test matrix for hover on the whirl tower involved thrust values from 0 to 44,480 N (10,000 lb) at several tip Mach numbers. Table 5 shows the test conditions for both rotors on

the whirl tower. For each rotor tested, the blades were tracked throughout the rpm range to be tested using a strobe-television system. The tracked and balanced blades were then subjected to the nominal conditions cited in Table 5. Performance and acoustic data were taken at each test point after the rotor environment became stable. The points were repeated several times. Wake-flow visualization was achieved through the smoke rake shown in Fig. 2. High-speed movies were taken of the smoke flow entrained by the rotor wake. In all hover performance cases, the ambient wind was less than 2 knots.

Flight Test Procedure

The flight testing of both standard and Ogee rotors on the UH-1H helicopter encompassed the major portions of the flight envelope for that aircraft. Those flight conditions which generated significant impulsive noise were of prime interest, but numerous other flight conditions were also explored. Table 6 shows the flight conditions for both rotors where all onboard data systems were acquiring data. Table 7 indicates the flight conditions over the acoustic array at Wallops Flight Center. During the acoustic-array data acquisition, the aircraft was flown only at its lower nominal gross weight of 33,805 N (7600 lb). The flight test conditions outlined in Table 6 contained at least 30 s of time-correlated data from all data systems. The conditions in Table 7 for the acoustic-array flyovers involved positioning the aircraft over the array and tracking the position with radar. Level flights over the acoustic array were done at 30 and 61 m altitude. Descending flights were commenced approximately 2100 m from the threshold of the runway and continued approximately 300 m past the threshold with a flightpath to put the helicopter at a nominal altitude of 122 m over the center of the microphone array. In general, at least two runs at each airspeed and rate of descent were flown during these flyover tests. Acoustic-array data were acquired during the entire approach and flyover for each run. Onboard data were taken during a 30-s period which included the time interval when the aircraft was directly over the array.

Discussion of Results

The results of the full-scale rotor tests described above are presented in three segments. Acoustic data are shown in Figs. 6 through 11. Vibration and loads measurements are presented in Figs. 12 and 13, while performance information in hover and forward flight is contained in Figs. 14 and 15.

Acoustic Data

Hover Acoustic Data

The overall sound pressure levels from the whirl-tower hover tests are shown in Fig. 6. Since blade-vortex interaction is not achieved in hover, these overall sound pressure levels represent rotational and broadband noise. The rotational noise from these rotors in hover has the expected trends with thrust and tip Mach number. It should be noted that the lower tip loading of the Ogee rotor results in a reduction of rotational noise level, as does the thin profile at the Ogee rotor's tip. Figure 7 shows a segment from high-speed smoke movies of both rotors' wake. The operating conditions on the whirl tower are nominal, and, as shown, develop tip vortices which exhibit characteristics similar to those seen from small-scale studies.[3] Specifically, the Ogee-tip vortex has a larger core and is less well defined in the lower wake. This vortex diffusion will be shown to affect the impulsive noise and blade loads.

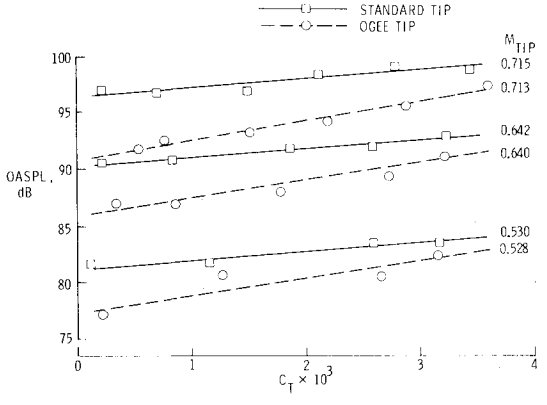

Fig. 6 Overall sound pressure levels for Ogee and standard rotor in hover.

Near-Field Rotor Noise

The noise perceived in a helicopter cabin and measured by external microphones is generated by several sources. Rotational noise and tail rotor noise are certainly contributors to the overall acoustic energy; however, impulsive noise in the near field below the rotor is dominated by blade-vortex interaction. The directivity of this type of impulsive noise as well as an explanation of its aerodynamic causes are given in several references.[6,7]

The test matrix for quantification of impulsive noise has already been described. From the onboard microphone data, peak levels of near-field impulsive noise below each rotor were found at conditions indicated in Fig. 8. The blade-vortex interaction impulsive-noise conditions for the standard rotor were moved to higher rates of descent for a given airspeed through the use of the Ogee rotor. This phenomenon may be due to the diffuse Ogee-tip vortex requiring a closer proximity to the succeeding blades to generate impulsive noise. Another possible explanation for this phenomenon is that the Ogee-rotor impulsive noise originates from the interaction of the blade with vortices of significant age.

As shown in Ref. 7, such vortex systems could intersect this rotor on the advancing side of the disk at fairly high rates of descent. In order for these interactions to predominate the impulsive noise for the Ogee rotor, these older vortices would have to be more intense than those generated within two rotor

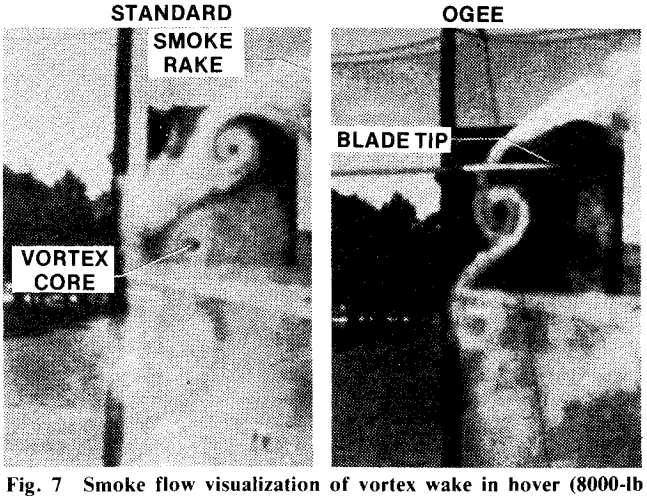

Fig. 7 Smoke flow visualization of vortex wake in hover (8000-lb thrust, 324 rpm).

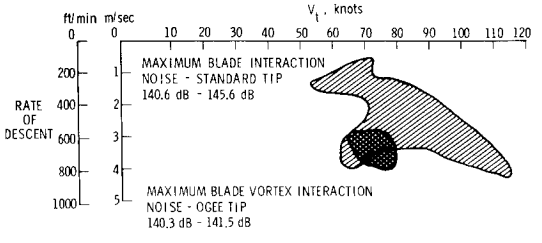

Fig. 8 Peak levels of near-field impulsive noise for nominal 7600-lb UH-1H as measured by IFAMS.

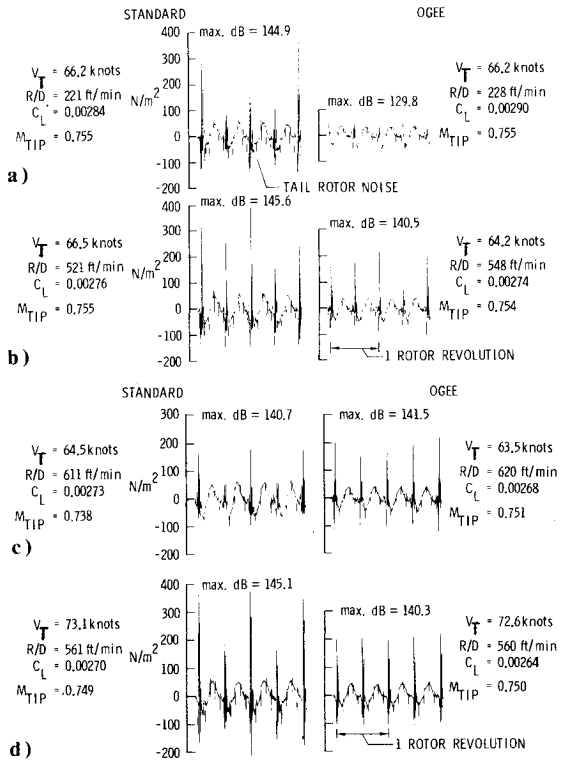

Fig. 9 Advancing-side microphone pressure time histories.

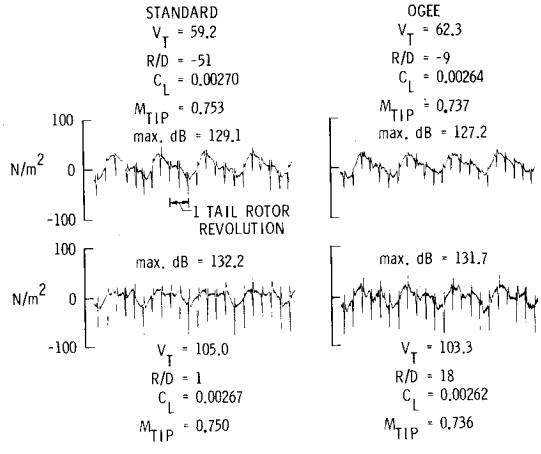

Fig. 10 Retreating-side microphone pressure time histories.

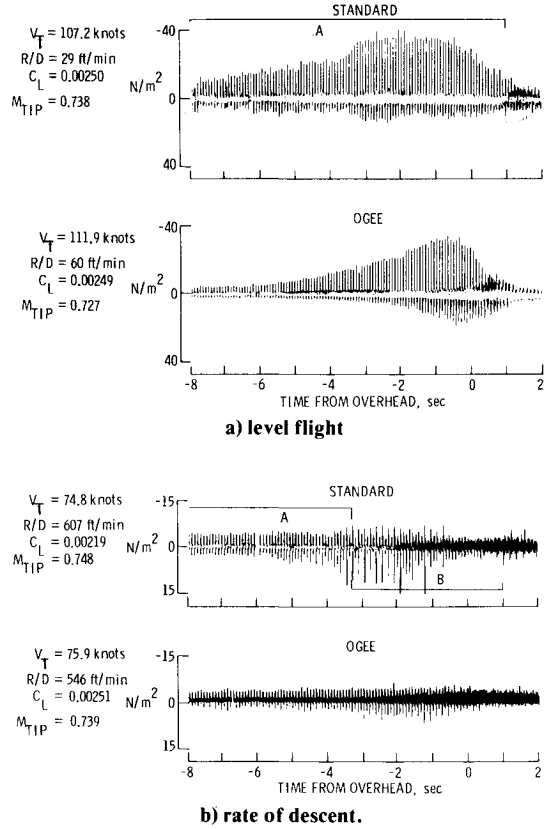

Fig. 11 Far-field rotor noise measured by acoustic-array center microphone.

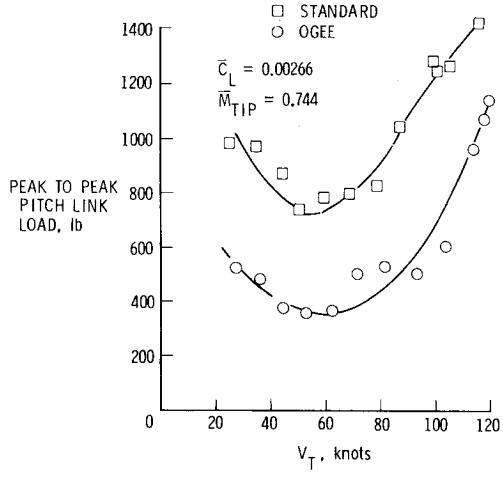

Fig. 12 Oscillatory pitch-link loads in level flight.

revolutions. Ray-tracing of the impulsive noise and forward-flight flow visualization would be needed to prove this hypothesis. It should be noted that the maximum intensity of the Ogee impulsive noise below the rotor is significantly lower than the maximum noise of the standard rotor.

The near-field acoustic data discussed in this section will be taken from these areas of maximum impulsive noise for both rotors. Time histories of data from the advancing blade microphone are shown in Fig. 9 for both rotors during rates of descent. The conditions chosen are those which were observed to bracket the strongest impulsive noise for both rotors. The strongest vortex-blade interaction occurs on the advancing side of the disk[7] and hence the advancing-side microphone data best illustrate the changes in such phenomena. The Ogee rotor significantly reduces this type of near-field impulsive noise as well as the rotational and tail rotor noise in rates of descent (see Fig. 9a). The rotational noise difference has been addressed in the last section. The tail rotor noise is a function of power required and, as will be shown, significant reductions in tail rotor power for the Ogee main rotor may be realized for some gross weights and flight conditions. Tail rotor interactions with the main rotor wake also cause changes in the acoustic signature of the tail rotor which are dependent on the wake's strength and trajectory.

The rotational and tail rotor noise can be more clearly seen in Fig. 10, which shows data from the IFAMS retreating-side microphone. These level flight data are free of main rotor impulsive noise. Again, changes in power required and tip loading between Ogee and standard main rotors probably account for acoustic differences.

Far-Field Rotor Noise.

Flight tests over an acoustic array result in data as shown in Fig. 11. These time histories show not only the acoustic phenomena illustrated in the near-field data, but also a significant addition to the acoustic energy, impulsive noise generated by compressibility. This very directional[6] noise is

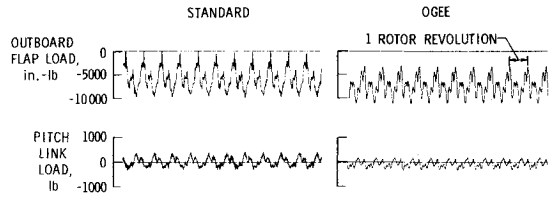

Fig. 13 Comparison of pitch link and outboard flap loads in descending flight (flight conditions of Fig. 9a).

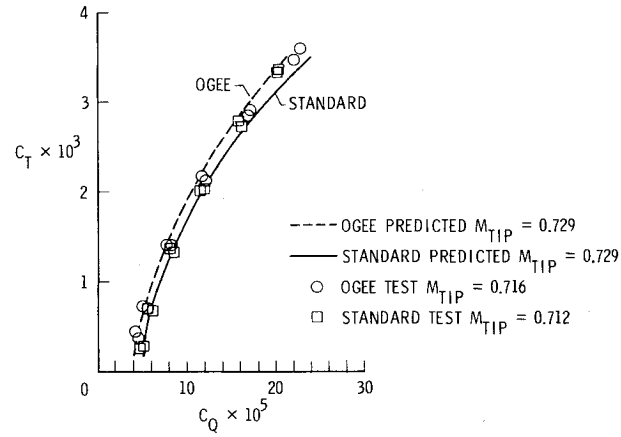

Fig. 14 Rotor hover performance at 324 rpm.

shown by area A in Fig. 11a for level flight at a nominal 61 m altitude. The aerodynamic cause of these negative pressure pulses is discussed in Refs. 6,7, and 8.

During rates of descent, the blade-vortex interactions generate the signature in area B of Fig. 11b. Note also that the compressibility spikes (area A) are still present. The trend of the vortex-blade interaction far-field noise with rates of descent and rotor tip shape is similar to near-field trends discussed earlier. The compressibility noise spikes (area A) for each rotor show differences which are magnified as aircraft speed increases. Figure 11a shows this for level flight where compressibility on the advancing blade is maximized. The thin profile of the Ogee rotor seems to decrease the magnitude of the compressibility impulsive noise.

Rotor Loads

The character of a rotor's structural loads is very dependent on the local aerodynamic environment. The rotating pitch-link loads of both Ogee and standard rotors are shown in Fig. 12 for level flight. The rotors are matched in C_T, ρ, and M_{TIP} within 2%. The marked reduction in peak-to-peak pitch-link loads for the Ogee rotor at this moderate C_T is probably due to a reduction in local tip chord.

Rates of descent during which blade-vortex interactions occur usually cause rotor flapwise loads and torsional loads to increase. Figure 13 shows the outboard flap load and pitch-link loads for Ogee and standard rotors during a rate of descent for which acoustic data has already been discussed. It may be noted that the harmonic content of these loads correlates with the strength of near-field impulsive noise. For the case where the standard rotor impulsive noise is greatest, the pitch-link loads and outboard flap loads contain many high harmonics. The Ogee loads for this case are considerably freer of high harmonics. The reduced blade oscillations probably result from a weaker tip vortex and accompanying interaction of that vortex with the following blades.

Rotor Performance

Hover Performance

The Ogee and standard rotor performance was predicted using a strip theory/momentum analysis. Uniform inflow and

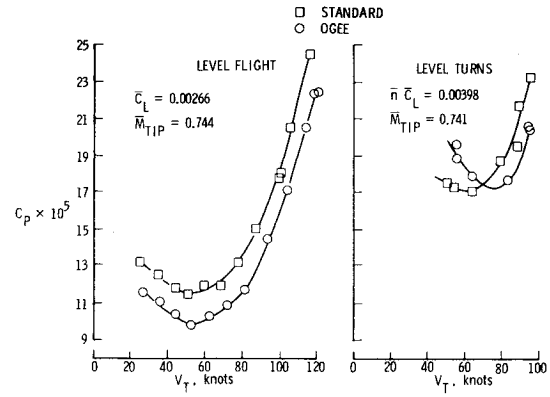

Fig. 15 Forward-flight performance of standard and Ogee rotors.

Mach number corrections were applied to a segmented rotor rotating at several tip Mach numbers. The predicted performance for M_{TIP} = 0.729 (324 rpm) is shown in Fig. 14. Preliminary results from tower-performance data confirm these trends at low and moderate thrust coefficients, while the test data for the two rotors merge at higher thrust coefficients ($C_T = 0.00275$). It should be noted that the simple momentum theory gives a better prediction of Ogee hover performance than for the standard. This might be due to the Ogee tip's diffuse vortex flowfield having less of an effect on the inflow in the tip region and thus more closely following the uniform inflow assumption of the theory. The improvement in performance at low and moderate C_T is due to a substantial decrease in torque-weighted solidity for the Ogee tip while thrust-weighted solidity is only moderately decreased.

Forward Flight

Level flight performance for standard and Ogee rotors as measured on the UH-1H aircraft is indicated in Fig. 15a for 33,805 N (7600 lb) nominal weight and 324 rpm. Thrust coefficients and tip Mach numbers were matched between rotors at a given airspeed within 2%. The difference in power coefficients at this moderate C_T is probably due to profile power differences between the two rotors. This power-coefficient reduction for the Ogee rotor corresponds to a maximum 135-hp savings over the standard rotor at standard sea level conditions. Performance data from nominal 1.5g level flight turns at various speeds are shown in Fig. 15b. At this higher thrust coefficient, the reduction in thrust-weighted solidity for the Ogee rotor is indicated by a reduction in performance gain over the standard rotor. At low speeds and high C_T, the data indicate a performance penalty for the Ogee rotor. Again, thrust coefficients and tip Mach numbers were matched between rotors as for 1g flight data.

Concluding Remarks

Full-scale tests were utilized to investigate the effects of the Ogee tip on helicopter rotor acoustics, loads, and performance. A whirl tower and instrumented UH-1H were used for this study. From the data analyzed to date, the Ogee tip changed the characteristics of the standard UH-1H rotor as follows:

1) The impulsive noise caused by vortex-blade interaction and compressibility was reduced for most flight conditions tested. Blade-vortex interaction noise was reduced by as much as 15 dB.

2) Rotational noise in hover was reduced throughout the thrust range tested.

3) Oscillatory rotor loads and control loads were reduced by as much as 50% and their harmonic content changed.

4) Forward-flight performance was significantly increased through use of the Ogee tip up to moderate thrust coefficients.

5) Preliminary hover performance results from the whirl tower indicate that the analytically predicted trends of Ogee-

rotor hover performance at moderate thrust coefficients may be realized. At higher thrust coefficients, the Ogee hover performance merges with that of the standard rotor.

6) The tail rotor noise was lower for many flight conditions with the Ogee-tip main rotor.

References

[1]Ward, J.F. and Young, W. H., Jr., "A Summary of Current Research in Rotor Unsteady Aerodynamics with Emphasis on Work at Langley Research Center," *AGARD Conference Proceedings No. 111 on Aerodynamics of Rotary Wings,* Fluid Dynamics Panel Specialists' Meeting, Marseilles, France, Sept. 13-15, 1972, pp. 10. 1-10. 20.

[2]Balcerak, J. C. and Feller, R. F. "Vortex Modification by Mass Injection and by Tip Geometry Variation," USAAMRDL, Tech Rept. 73. 45, June 1973.

[3]Landgrebe, A. J. and Bellinger, E. D. "Experimental Investigation of Model Variable-Geometry and Ogee Tip Rotors," NASA CR-2275, Feb. 1974.

[4]Balcerak, J. C. and Feller, R. F., "Effect of Sweep Angle on the Pressure Distributions and Effectiveness of the Ogee Tip in Diffusing a Line Vortex," (Rochester Applied Science Associates, Inc., Rept. 73-07; NASA Contract NAS1-12012), NASA CR-132355, 1973.

[5]Rorke, J. B. and Moffitt, R. E., "Wind Tunnel Simulation of Full Scale Vortices," NASA CR-2180, March 1973.

[6]Schmitz, F. H. and Boxwell, D. A., "In-Flight Far-Field Measurement of Helicopter Impulsive Noise," *Journal of the American Helicopter Society,* Vol. 21, Oct. 1976, pp. 2-16.

[7]Tangler, J. L., "Schlieren and Noise Studies of Rotor in Forward Flight, " Preprint 77.33-05, 33rd Annual National Forum of the American Helicopter Society, (Washington, D.C.), May 1977.

[8]Farassat, F. "Theory of Noise Generation from Moving Bodies with an Application to Helicopter Rotors," NASA TR R-451, Dec. 1975.